SOLUTION MINING RESEARCH INSTITUTE

105 Apple Valley Circle
Clarks Summit, PA 18411, USA

Telephone: +1 570-585-8092
www.solutionmining.org

Technical Conference Paper

Ground deformation mapping and monitoring of salt mines using InSAR technology

Violeta Velasco, Ciscu Sanchez,
TRE ALTAMIRA S.L.U
Ioannis Papoutsis, Sylvia Antoniadi, Charalampos Kontoes,
National Observatory of Athens (NOA)
Dorothea Aifantopoulou, Sideris Paralykidis,
GEOAPIKONISIS S.A.P.GE.

SMRI Fall 2017 Technical Conference
25 - 26 September 2017
Münster, Germany

Solution Mining Research Institute Fall 2017 Technical Conference

Münster, Germany, 25 - 26 September 2017

Ground deformation mapping and monitoring of salt mines using insar technology

Abstract

InSAR technology can be used for monitoring surface deformation caused by mining operations, both open pit and underground mines, worldwide. This technology allows the systematic mapping of all ranges of motion (millimetric, centimetric and metric magnitudes) over extremely large areas with a high density of measurement points.

Mining assets can be monitored regularly and precisely to record possible deformation patterns, assess the site's deformation regime and issue alerts upon initiation of new movements in terms of magnitude and spatial characteristics. In addition, this technology is especially useful in abandoned mining areas, where continuous and in-situ monitoring is not carried out anymore while information about the ground motion is still required.

To illustrate the capabilities of this technology, a recent case will be presented, referring to the elaboration of ground deformation maps for the Solotvyno salt mine area in Ukraine. The aim of the study was to delineate subsiding areas and unstable slopes, and to identify risk-sectors prone to landslides and other ground failure phenomena, such as major ground collapses that have created giant sinkholes very close to populated areas in Solotvyno.

Peristent Scatterer Interferometry analysis was conducted for Solotvyno mines area, in the context of two monitoring modes: (1) Historical Analysis from 1998 to 2016 with the C-band satellites ERS, ENVISAT and Sentinel and (2) 2016 - 2017 Monitoring using the high-resolution X-band satellites Cosmo-SkyMed. Additional information was properly integrated into this analysis, such as geographical and geological data, and assets extracted from very high resolution optical satellite imagery. As a result, subsidence and landslide risk areas for each study period were adequately classified. The thematic maps and geospatial databases that were produced, outline several critical zones in the mining area requiring immediate attention of decision makers and showcase the value of consistent and seamless monitoring of abandoned mines.

This study was elaborated in the framework service contract N. 259811, for the Risk & Recovery leg of the Copernicus Emergency Management Service, on behalf of the Hungarian National Directorate General for Disaster Management that participated to the Scoping Mission in Solotvyno mine.

Key words: Solotvyno salt mine, InSAR technology, abandoned mines, risk maps

1. Introduction

Abandoned mines and their associated hazards can pose major threats to local communities and the environment. This worldwide problem is the result of the extraordinary mining development that took place in specific areas in the late 19th and early 20th centuries.

Whereas active mining operations are mostly well monitored, the approach when the mine is no longer profitable and is abandoned can vary from country to country. Following the closure of a mine, the awareness of previous mining activities often decreases but former mine shafts and underground cavities, re-filled open pits, tailings and dumping sites still exist (García, 2017).

Additionally, it has to be highlighted that the challenges of post-mining in terms of economics, environmental or social aspects must not be postponed to the phase after the mine closure (Melcher, 2017) in order to improve the hazards mitigations.

Hazards requiring mitigation can include collapses migrating to the ground surface: sinkholes, slope instabilities and collapses, subsidence or uplift of the ground surface.

Most mining authorities have similar information needs. The common steps to evaluating the risk are: mapping and assessing the hazard, identifying the exposure of people and infrastructure, and monitoring the hazard with a frequency dependent on the magnitude of the hazard and the risk posed.

An important addition to existing monitoring techniques, which is generating considerable interest among mining local administrators and other responsible authorities today, is the ability to monitor the surface deformation over the entire mining area from space. This is achieved through Interferometric Synthetic Aperture Radar (InSAR) (Graniczny et al., 2013).

Compared to other surveying techniques, InSAR has the advantage of providing high density of measurement points over large areas, including areas that are dangerous or difficult to access e.g. in (Sánchez et al, 2016a, Sánchez et al, 2016b and Raventós et al., 2017). Advanced InSAR techniques developed in the last decade, provide millimetric precision time series of movement.

Other advantages of measuring ground motion with this technology are: (1) the stability of all key elements of the mine site can be monitored at the same time: slopes of the open pit, ground deformation of waste piles and surrounding areas, leach pads, tailing ponds, access roads; (2) It helps to predict which areas and infrastructures are most likely to be vulnerable to failures aiding the planning of risk mitigation measures and (3) the integration and validation of the InSAR results with further valuable data (e.g. geological, operational, geotechnical, etc.) significantly improve the methodology for establishing the risk assessment of active and abandoned mines. Thus, the combination of data provides the possibility to make a comprehensive estimation of subsidence and landslide risk, considering the evolution of the risk in time.

This technology has been proved to be an effective instrument to improve the identification and delimitation of moving areas associated to mining activities in a great number of studies. For instance, this technology has been used to monitor from precursory and slow millimetric motion to high magnitude (decametric and metric) and fast motion in the mining environments (e.g. Pryzlucka et al., 2015, Pinto et al., 2017). Related with post-mining this technology has been used in a wide number of mining case studies and non-active mine assets such as old waste dump areas, inactive open pits and slopes measuring and providing reliable information of the residual motion and post-mining behavior may have caused by past mining activities. Some cases studies regarding abandoned mines across Europe were analyzed during the Terrafirma GMES Service Element project 2003-2009 (for further information please see the publication Adam, et al 2009). Other project related with Salt mining environments were performed in the active large salt underground exploitations in the central Catalonian Basin, northeast Spain.

In the light of the aforementioned discussion, the objective of this paper is twofold. First, we present the application of InSAR technology for providing valuable insights in the methodology of monitoring of abandoned mines areas. Second, we present and discuss the implementation of this methodology to delineate subsiding areas and to identify risk-sectors for the Solotvyno salt mine area in Ukraine. Is should be noted that the framework presented can be applied for monitoring further mining areas.

2. Area of Interest

2.1. Geographical and Geological settings of the study area.

Zakarpattya is a region with the unique geopolitical and geographical location, covering the south-west part of the Ukrainian Carpathians and Dunabe lowland. This is a sole region of Ukraine, which borders with 4 countries such as Hungary, Poland, Romania and Slovakia.

Zakarpattya has the bowels rich in various minerals, including specific ones, typical only for Zakarpattya geological province. The mineral base of the region is represented by almost 150 deposits and more than 30 minerals.

Great focus is paid to subsequent structural development of national economy complex, attraction of national and foreign investments in the economy, development of small and medium business, and effective use of natural resource potential. The high-quality new pre-conditions for regional economic development appeared with realization of conception of the free economic zone "Zakarpattya" and introduction of the special regime of investment activity of the region’s territory. Almost 400 enterprises

with foreign investments were registered; over one thousand joint ventures operate (Source: Ministry of Foreign Affairs of Ukraine[1]).

Solotvyno (Figure 1) is an urban-type settlement in Tiachiv Raion in Zakarpattia Oblast of Ukraine, located close to the border with Romania, on the right bank of the Tisza River (across from the Romanian city of Sighetu Marmaţiei).

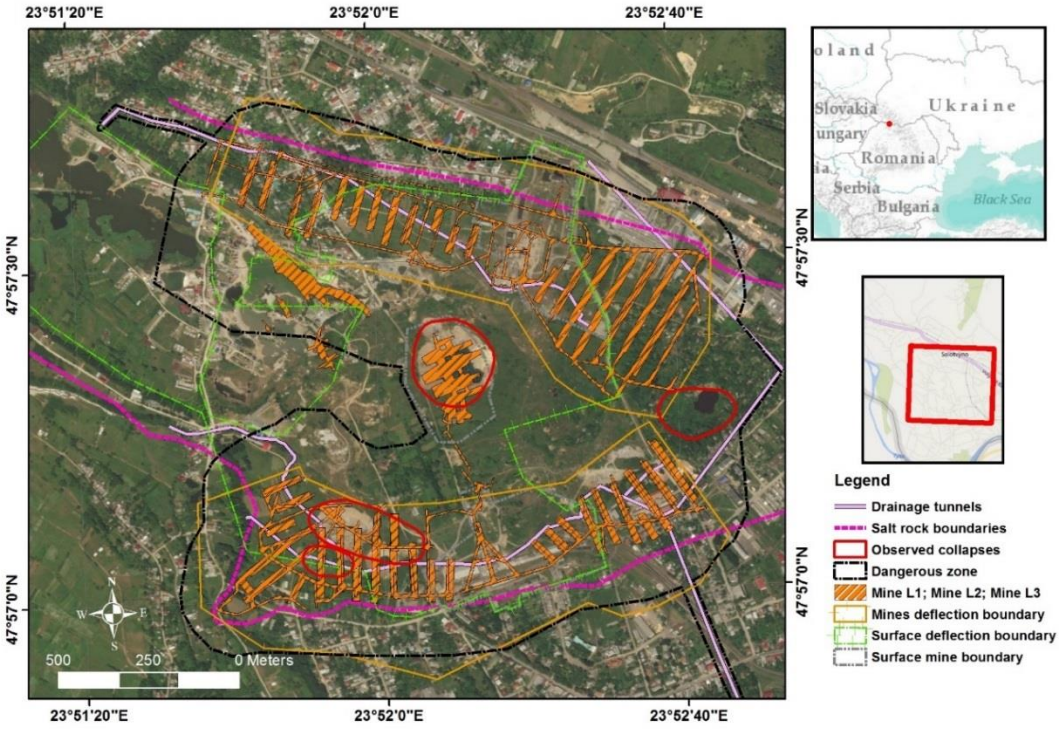

Figure 1. Solotvyno mines on the map.

Since the second half of the 18 th century Solotvyno began to build the mines. Since then it has put into operation nine mines, although during the last decade, there only two: the eighth and ninth (Figure 2). In the 60-70's at a depth of 300 meters (984 feet) even opened two allergological hospitals. In the underground salt chamber, with a unique microclimate, patients came to be treated for asthma and allergies. In parallel Solerudnik regularly mined salt. The first major collapse due to underground works appeared in 1973 in the center of the mining area.

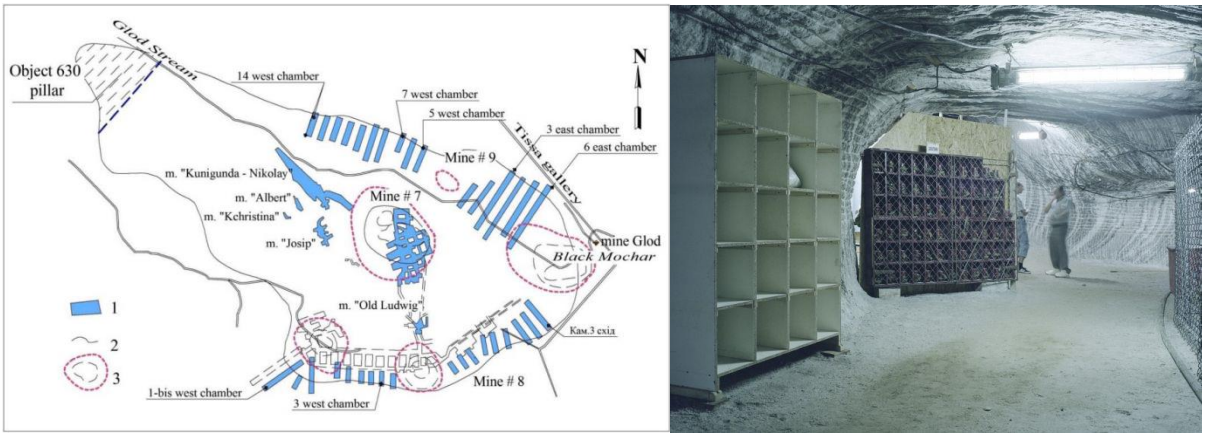

Figure 2. (left) Location of different mining sites in the AOI (source: Report 1 - Ref. Ares(2016)4085429 - 03/08/2016), (right) one of the salt mines in the town of Solotvyno (Photo credits: Kirill Kuletski).

In the late 90's water entering a tunnel exhaust washed the salt, creating huge underground karst cavities in which the soil collapsed. The largest crater was formed above the mine № 7 (Figure 2). The experts have established that the perimeter and depth of failure increased with a speed of 1-2 meters (3.2 – 6.4

[1] http://mfa.gov.ua/en/about-ukraine/info/regions/7-uzhgorod

feet) per week. The main threat was the enhancement of one of the holes in the side of a residential village. Experts warned that if the mine number 9 were to be filled with water to a critical level, it would lead to unpredictable destructive underground processes.

In December 2004, the Ukrainian Cabinet made the state enterprise "Solotvinskiy pit" to the list of enterprises of strategic importance to the economy and national security. Underground mines have also made the list of high-risk businesses, the discontinuation of which required special measures to prevent damage to the life and health of the citizens and the environment.

Since 2011, there is no longer any mining activity on the site. All active mines have been abandoned following their flooding. Other large collapses appeared at that time in the south and north of the mining area. The depth of underground mines varies from 30-40 m (98-131 feet) to about 400 m (1310 feet), from the center to the perimeter of the mining area. No relevant and reliable information on precise position, organization, dimensions of mining underground are available.

The sinkholes in Solotvyno present the following potential:

- Total volume of mine workings consists of about 15.5 million m^3 (547 million $feet^3$).
- Total volume of karst cones (2015y) is about 6 million m^3 (211 million $feet^3$) with surface of about 0.25 km^2 (299.000 $yards^2$).
- The reserve of increasing of the total karst'(subsidence) volume and surface is considered large enough.
- Maximum rate of increasing of karst cones' volume and surface were observed between 2011 and 2013 is 1.3 million m^3/year (45 million $feet^3$/year) and 35.000 m^2/year (41.800 $yards^2$/year) respectively.

The village, which stands on a giant salt dome, according to experts contains 250 million tons of salt. Sinkholes in the region are caused by the salt mines abandoned and left to collect water underground. The collected water dissolves underground rock formations and leaves huge caverns when it eventually drains away. The empty cavern eventually collapses causing vast sinkholes.

Recently, there are two main subsidence expressions in the Area of Interest (AOI) that is a direct result of the regional mining activities. These are:

Large collapses with a diameter up to 200 meters (656 feet) and with a depth of about 20-30 meters (65.6 – 98 feet). In 2015 a hole measuring 100 meters (328 feet) wide and 60 meters deep (196 feet) (Figure 3), suddenly opened up in the village of Solotvino in the Zakarpatska Oblast region of western Ukraine.

Figure 3. Huge collapses appearing the village of Solotvyno in the Zakarpatska Oblast region of western Ukraine (source: http://www.independent.co.uk)

In 2011 a circular hole opened up. This crater has grown so that in 2016 it now has an elongated shape with a surface area that is at least three times greater.

Sinkholes that are smaller collapses with a funnel shape of about 10 meters (32 feet) in diameter. These collapses, in a first approximation can be considered as a sudden soil movement with no prior warnings. These collapses are likely induced by the dissolution and the karstification located at the top of salt deposit at about 30 m (98 feet) deep. This dissolution can likely induce slow movements of subsidence covering the entire area with an expected magnitude of subsidence in the order of cm to dm per year. The most recent sinkhole was generated in 2015, while two more similar collapses took place in 2011 and 2012.

The sinkholes generation risk led the Directorate General for European Civil Protection and Humanitarian Aid Operations of the European Commission (DG ECHO) to organize a four-day scoping mission between 4-7th of July 2016 to Solotvyno, where the abandoned and neglected salt mine poses a significant contamination threat of the Tisza River and also threatens the livelihoods of those living in the region.

2.2. Material and Methods

2.2.1. Data

For this project, a wide range of spatio-temporal data of different nature (e.g. geological, geographical, geotechnical, etc.), from different sources (e.g. remote sensing, other databases, etc.) and different formats were collected, harmonized, geo-referenced, quality-checked and duly corrected and updated. In the following paragraphs, a brief description of the main data used for this study is presented:

- **Geo-Spatial Data:**

  The following data were integrated in the processing.

  (1) EO optical Data: A *Pleiades* image (acquired the 12/07/2015) was used to generate adequate geospatial data, after being orthorectified.
  (2) Open data: Their integration refers mainly to geometry and attribute information homogenization and gaps filling:

  - DEM || SRTM 1 Arc-Second Global. (USGS),
  - Administrative Boundaries || Global Administrative Areas (GADM)
  - Transport Network, Hydrologic Network & PoIs || OpenStreetMap (OSM)
  - Geo-portals (Google Maps, WikiMapia, Google Earth)
  - Meteorological Data || NCEP (National Centers for Environmental Prediction)
  - CLC layer covering the Romanian part of the AOI

  (3) Other Data: Their integration refers mainly to digitization & extraction of attribute information and/ or co-registration:

  - Mines data. Scoping Mission in Solotvyno mine - Ukraine / National Directorate General for Disaster Management - Hungary (EUCPT / NDGDM): 3 different maps were geo-referenced (using the Pleiades optical imagery for GCPs collection), and digitized in a GIS environment. The geometry of the boundaries of the underground salt mines, the underground and surface deflection boundaries, the salt rock boundaries and the centerline of the drainage tunnels was established (Figure 2).
  - ESRI Basemap / World Imagery[2] (ESRI / ArcGIS)

  (4) Generation of Additional Layers:

  - Ground Movements. Using the available optical imagery and through photo-interpretation, the boundaries of collapses, sinkholes and landslides were digitized for the year of 2015.

[2] http://goto.arcgisonline.com/maps/World_Imagery

- LULC layer. The CLC layer covered the Romanian part of the AOI, only. Moreover, the MMU of 25ha not fitting with the scale of the final products (1:4.000), the AOI LULC layer was produced, via photointerpretation of the optical VHR satellite imagery.
- Digitization of Buildings Footprints (BFs). These were digitized on the basis of the available optical VHR satellite imagery information.
- Contour lines & height spots. These were produced through a semi - automated approach, using as input file the SRTM 1-arc second data set.

- **Radar Data:**

For achieving the objectives of this project, several sets of radar images acquired from medium resolution satellites (C-band) such as ERS, ENVISAT-ASAR and Sentinel were used for performing historical analysis. Additionally, a high-resolution satellite band (X-band) such as Cosmo-SkyMed satellites were used for covering the most recent time span. The spatial resolution and the number of images used from each satellite is showed in table 1.

Period	Satellite	Geometry	Spatial resolution (m) [feet]	Number of images*	Minimum Revisiting Time
January 1997 – January 2001	ERS	Descending	4 x 20 [13 x 65]	29	35
October 2002- October 2010	ENVISAT	Descending	4 x 20 [13 x 65]	30	35
October 2014 – September 2016	Sentinel	Descending	20 x 5 [65 x 16]	44	12/6
October 2016 – February 2017	Cosmo-SkyMed	Descending	1 x 1 [3.2 x 3.2]	25	11

Table 1: SAR dataset over the Area Of Interest.

In the following paragraphs, further details of the radar satellite data are described:

- **ERS 1997-2001:**

A descending dataset included 29 images acquired on Track 50, frame 2637 covering the time period from 1997-2001 were selected.

- **ENVISAT-ASAR 2002-2010**

For the sake of continuity with the ERS dataset, the descending pass has been used. Thus, 30 images have been acquired on Track 322 for the frame 2637 covering the time period comprised between 2002 and 2010. It should be noted that for year 2001 no suitable satellite SAR imagery exists, due to the onboard failure of the gyroscope in ERS-2.

- **SENTINEL-1A 2014-2016**

A descending Sentinel-1A datasets (C-band) including 44 images on Track 80 for the time period between October 2014 and September 2016 have been used. Figure 4 shows the temporal distribution of ERS images corresponding to the descending orbit.

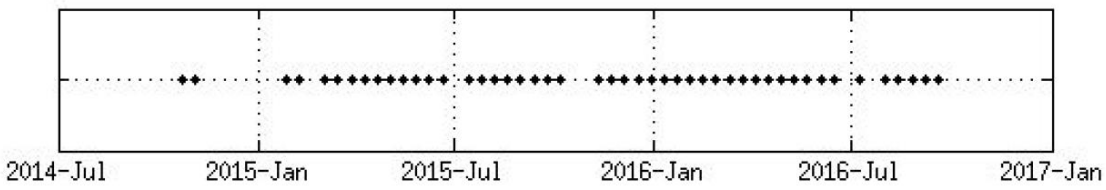

Figure 4.Temporal distribution of Sentinel acquisitions for the descending orbit (EMSN-030, 2016).

- **Cosmo-SkyMed 2016- 2017**.

Finally, the high-resolution satellite (X-band) Cosmo-SkyMed (CSK) has been used for performing a recent historical analysis. The CSK spotlight dataset include 25 images for a period of 4 months from October 2016 to February 2017.

2.2.2. Methods

In order to delineate the subsidence and landslide risk zones over the Area of Interest, we have analyzed the radar data and we have integrated these results with the rest of the data for a subsequent processing. In the following paragraphs, the main aspects of the InSAR-based methodology used to analyze the radar satellite data and the procedure for obtaining risk thematic maps is described.

- **InSAR methodology:**

Radar satellites use a form of active remote sensing termed Synthetic Aperture Radar (SAR) to obtain ground surface information. By actively emitting microwaves frequencies and recording the reflected signal, SAR systems capture highly precise information on the location of the features on the ground surface. These radar satellite can operate continuously through the day and night and in nearly all-weather conditions. The signal emitted by the SAR system is of a specific wavelength, meaning that the signal echoed (reflected) from a unique point on the ground and recorded by the radar satellite contains many returning radar pulses, including the fraction of the current wave cycle (phase) and the reflection strength of the signal (amplitude). When the ground surface changes, the distance between the sensor and the ground changes, which produces a corresponding change in measured signal phase. These changes in the measured phase value is used to quantify ground movement. Interferometric Synthetic Aperture Radar (InSAR), is the measurement of signal phase change over time. Differences in the signal phase values recorded between successive radar images are represented in an interferogram, which provide movements detection of the ground surface. However, there are some contributing factors that also impact phase shift such as topography and atmospheric interference, which limits the accuracy of measured ground movement to centimeter scales (from Falorni et al., 2011).

In order to overcome these limitations, a new trend emerged with the evolution of Advanced DInSAR (A-DInSAR) techniques, which are based on the processing of temporal series of SAR data to form time series of deformation (Paradella et al., 2015). Over the past two decades, InSAR techniques evolved from the use of differential interferograms (DInSAR) in the late 1990s (Massonnet et al., 1998) to persistent scatterers interferometry (PSI) in the early 2000s (Ferretti et al., 2001; Werner et al., 2003; Costantini et al., 2008). PSI overcomes limitations related to the atmospheric contributions affecting the standard DInSAR technique .Moreover, PSI techniques can retrieve a high number of measurements points from natural reflectors located on the Earth's surface when no big changes occur during the period of study. The combination of different SAR processing techniques guarantees the best measurement precision for all ranges of motion, from millimetric to centrimetric magnitudes (in Colombo et al., 2015).

PSI techniques such as PSInSAR identifies individual pixel with strong signal returns referred as Permanent Scattereres in order to measure surface movement occurring through the time (Ferretti et al., 2001). These PS are limited in distribution to rocky terrain or more urban settings. To improve the technique under other surface conditions, such as those found in and around mining operations a more complex scattering model was needed. Distributed scatterers (DS) are low-amplitude but coherent returns that are identified on a pixel-by-pixel basis. *The better temporal and spatial resolution of the new satellites improved the signal-to-noise ratio to the point where these DS became a significant contributor to the deformation monitoring signal. Advanced processing that optimizes the PS and DS*

returns, such as SqueeSAR™, were developed to provide displacement information not only on man-made structures or exposed rocks, but on outcrops and thinly vegetated areas (in Colombo et al., 2015).

The basic algorithm behind SqueeSAR™ has been outlined in Ferretti et al., 2011 and further discussed in an EAGE publication (Ferretti, 2014).

For each ground point, the following principle information is supplied using SqueeSAR:

- Position on a reference map;
- Average displacement rate [mm/yr and inches/yr] of the ground point, with precision that can exceed 1 mm/year (0.03937 inches/yr);
- Time-series of ground point displacement [mm], with accuracy that can exceed 5 mm (0,19 inches);
- Elevation value [m].

In order to successfully perform a SqueeSAR™ analysis, a minimum number of satellite images (approximately 15-20) are required over the same area of interest (AOI). This is necessary to create a reliable statistical base of electromagnetic ground point responses, used to identify which pixels contain usable information and which contain noise. The higher the number of images acquired and processed, the better the results obtained. All measurements provided are taken in the Line-of-Sight (LOS) direction meaning that measurements are a projection of the real motion into the detection vector or looking vector of the satellite called the Line-of-Sight.

- **Risk Maps-Thematic Maps**

Delineating subsidence and landslide risk zones over sparsely distributed Persistent Scatterers is challenging. Using a best fit surface can lead to reduced thematic accuracy of the final product, with several omission and commission errors. Hence, for delineating the subsidence risk zones we adopted a three-step approach:

1. The risk delineation was not done using the final PSI product, but based on a strictly qualitative product, as the one depicting in Figure 4. This is an intermediate product in the PSI processing chain and contains several atmospheric, orbital errors, etc. when it comes to absolute measurements. However, it serves as very good indicator of the major subsidence and uplift areas, in qualitative terms.
2. Upon producing the risk polygons based on the previous step, then the polygons were reclassified based on the average slope, to subsidence and landslide risk areas.
3. Finally, each polygon was classified to Low, Moderate or High risk, depending on the average deformation rate of the actual Persistent Scatterers lying within the polygon itself.

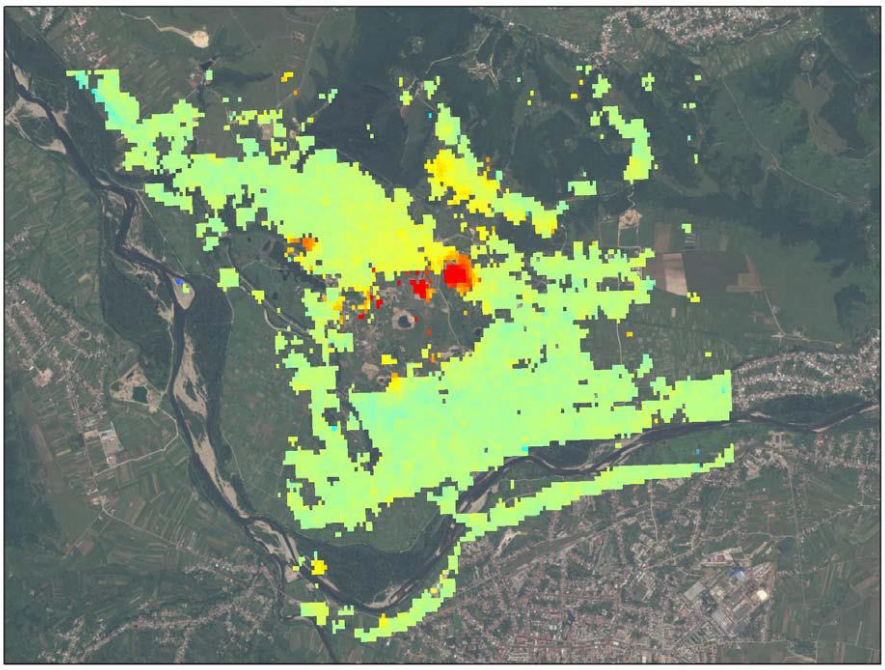

Figure 4. Qualitative information used to drive risk delineation. The color scale goes from light blue (uplift) to dark red (subsidence).

3.1. InSAR results:

- **ERS (January 1997 to January 2001).**

Over 1593 unique PS points and DS points representing line-of sight movements were identify from a SqueeSAR analysis. The figure 6 shows the mean annual deformation map for Solotvyno area of interest coming from the ERS satellite data analysis. The map shows the spatial distribution and the mean annual velocity value of the measurement points obtained. The velocity value, in mm/yr, and the point color are set according to the scale presented in the map.

A main pattern of deformation was detected in the vicinity of the sinkhole area with deformation values ranging from approximately -5 mm/yr (-0.19 inches/yr) in the outer zones (time series in fig 7) and up to 20 mm/yr (0.78 inches/yr) in the inner areas closer to the sinkhole (time series in fig 8).

Time series examples in the figures 7 and 8 shows how the motion is quite linear, in particular in the inner areas closer to the sinkhole.

The averaged standard deviation of the velocity for the measurements is about 0.6 mm/yr (0.023 inches/yr) in velocity and 93 % of measurement points are under +- 5 mm/yr (+- 0.19 inches/yr) motion during the time span of the historical study (1997 and 2001).

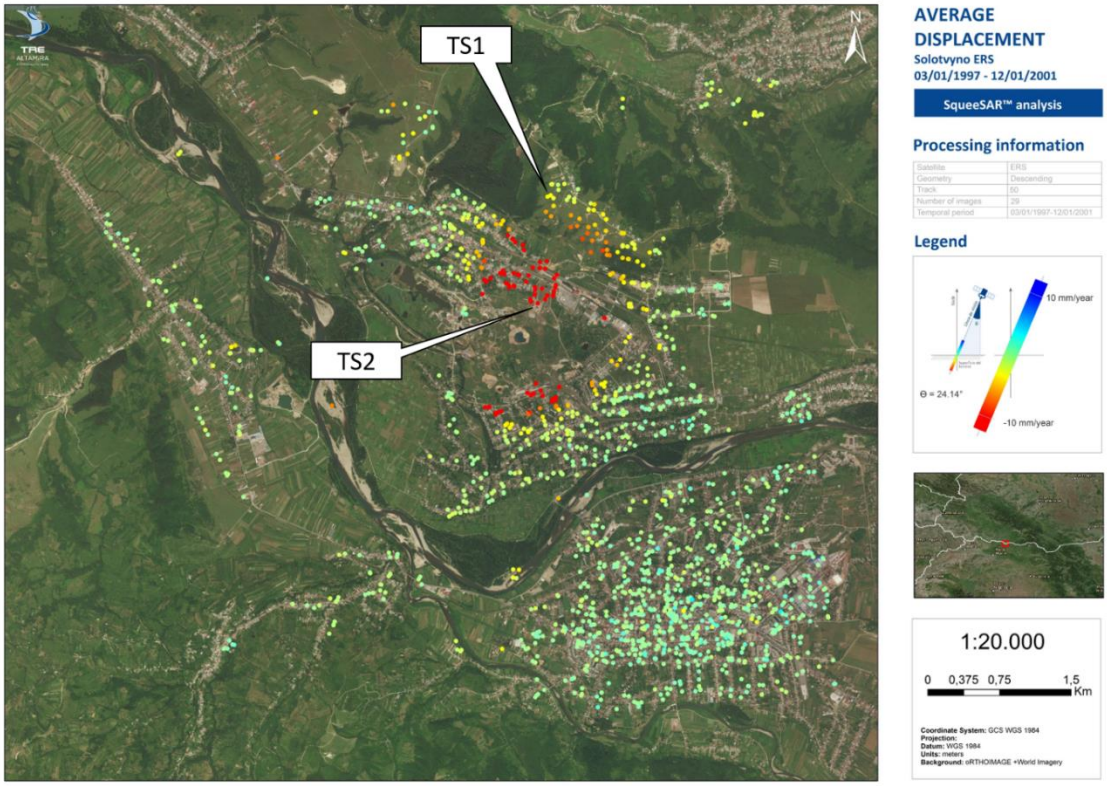

Figure 6: Mean annual deformation map from ERS data in the period January 1997 – January 2001.

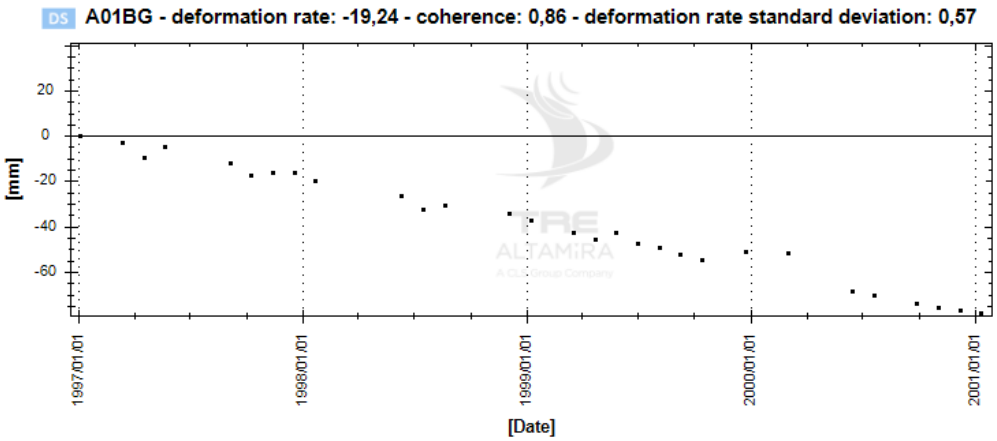

Figure 7: Time series TS1 from the ERS ground deformation analysis

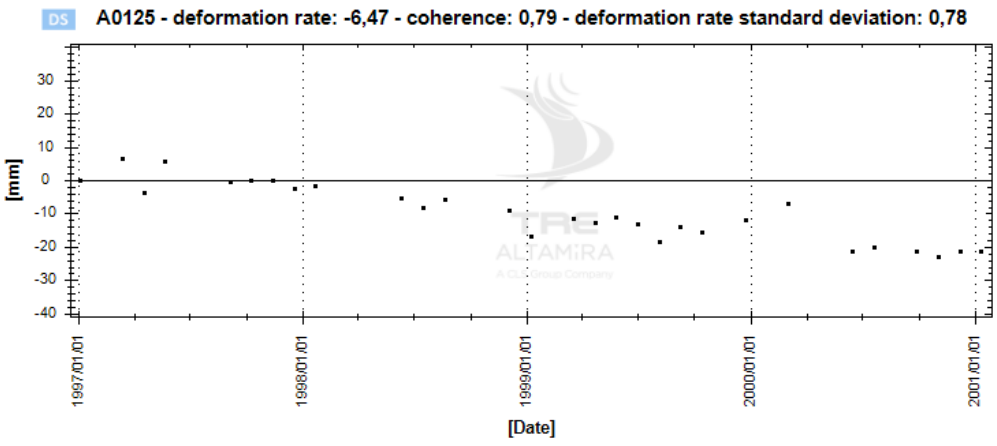

Figure 8: Time series TS2 from the ERS ground deformation analysis

- **ENVISAT (January 2003 to October 2010).**

Over 1627 unique PS points and DS points representing line-of sight movements were identify from a SqueeSAR analysis. The figure 9 shows the mean annual deformation map for Solotvyno AOI coming from the ENVISAT satellite data analysis. The map shows the spatial distribution and the mean annual velocity value of the measurement points obtained. The velocity value, in mm/yr, and the point color intensity are set according to the scale presented in the map.

Mean annual deformation was computed using data from January 2003 to October 2010. A clear pattern during this period is detected mainly in the north of the sinkhole area. Values ranging from 4 or 5 mm/yr (0.19 inches/yr) to 25 mm/yr (1 inch/yr) in the vicinity of the sinkhole are detected.

Time series in the following figures, 10 and 11, show the evolution and trend of the deformation of two example locations, shown in figure 9, detected in the ENVISAT analysis.

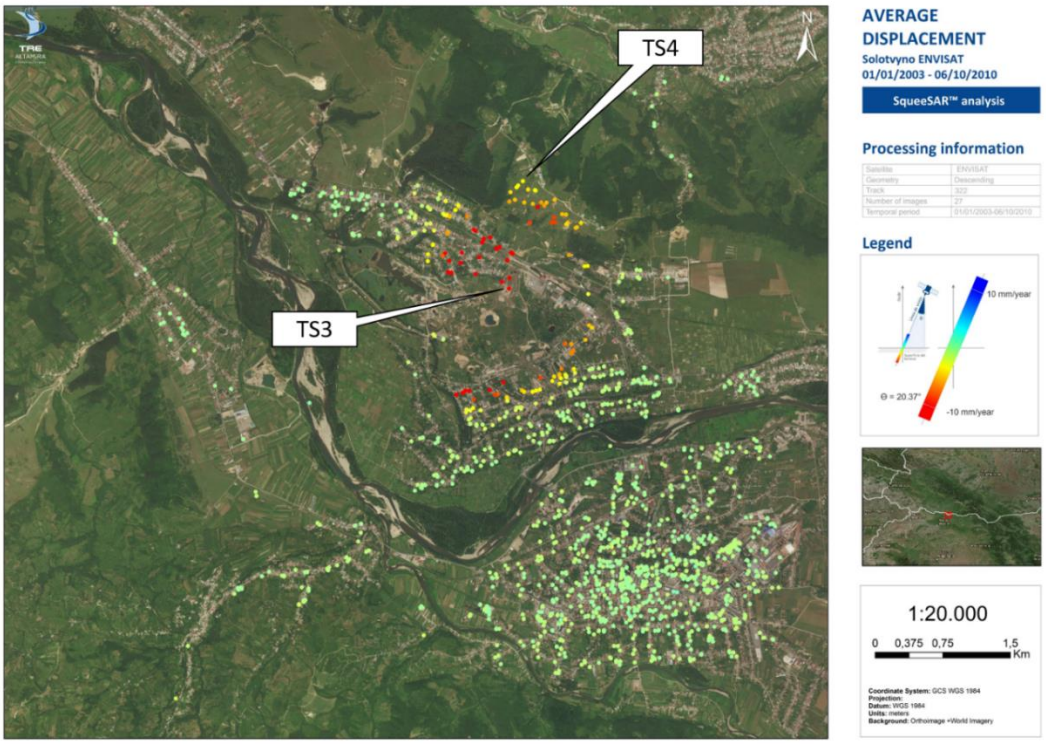

Figure 9: Mean annual deformation map from ENVISAT data in the period January 2003 – October 2010.

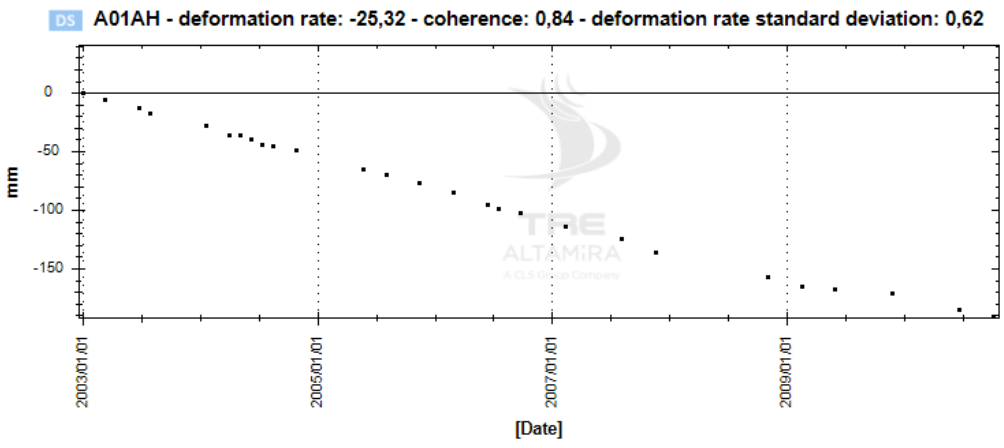

Figure 10: Time series TS3 from the ENVISAT ground deformation analysis

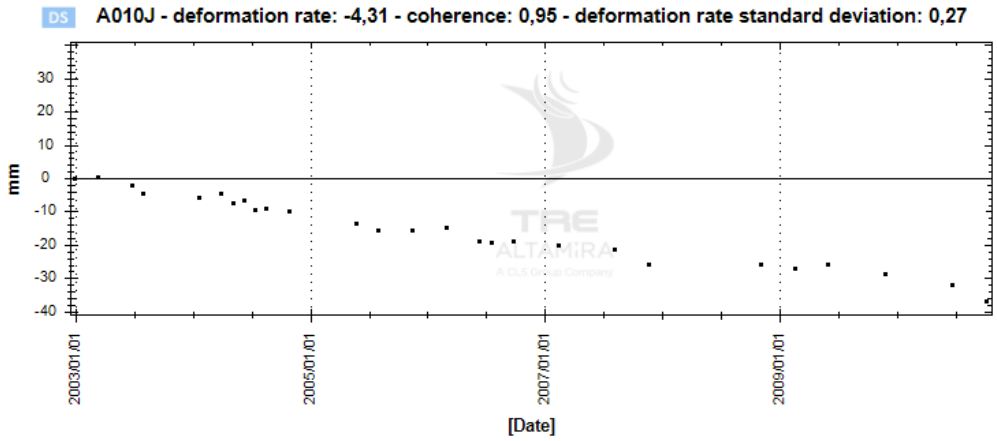

Figure 11: Time series TS4 from the ENVISAT ground deformation analysis

- **Sentinel (October 2014 to September 2016).**

Over 7411 unique PS points and DS points representing line-of sight movements were identify from a SqueeSAR analysis. The figure 12 shows the mean annual deformation map for Solotvyno area of interest coming from the SENTINEL satellite data analysis. The maps shows the spatial distribution and the mean annual velocity of the measurement point obtained. The velocity values, in mm/yr, and the point color intensity are set according to the scale presented in the map.

A SENTINEL dataset covering a period from October 23rd to September 18th was used for the detection of mean deformation in the area of interest. Deformation is focused in the vicinity of the sinkhole area. Higher deformation rates are located at the northeast sector of the sinkhole which presents magnitudes up to 25 mm/yr (1 inch/yr). A clear pattern coming from the north to the sinkhole inner area is detected with a visible increase in the velocity up to 6 mm/yr (0.23 inches/yr).

Time series examples in the figures 13 and 14 show the evolution of the motion which is very linear in both time series presented.

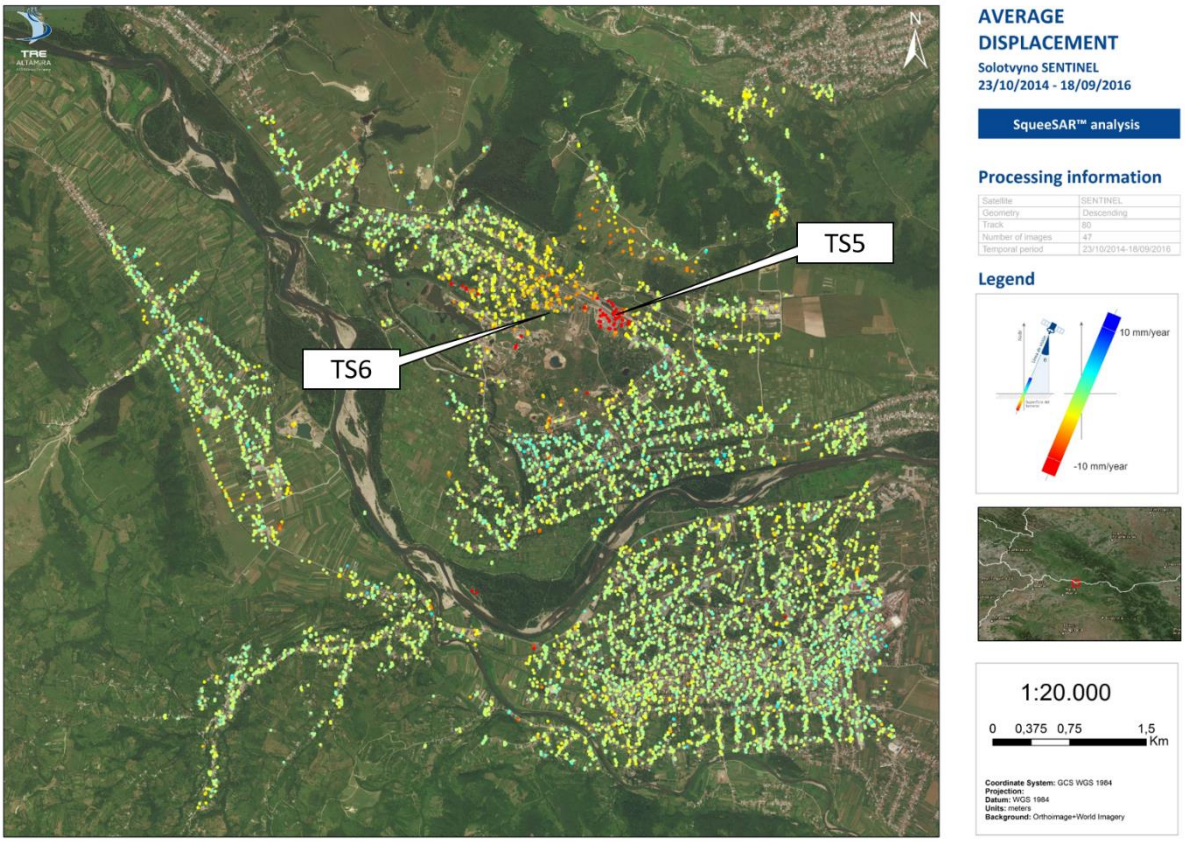

Figure 12: Mean annual deformation map from SENTINEL data in the period October 2014 – September 2016.

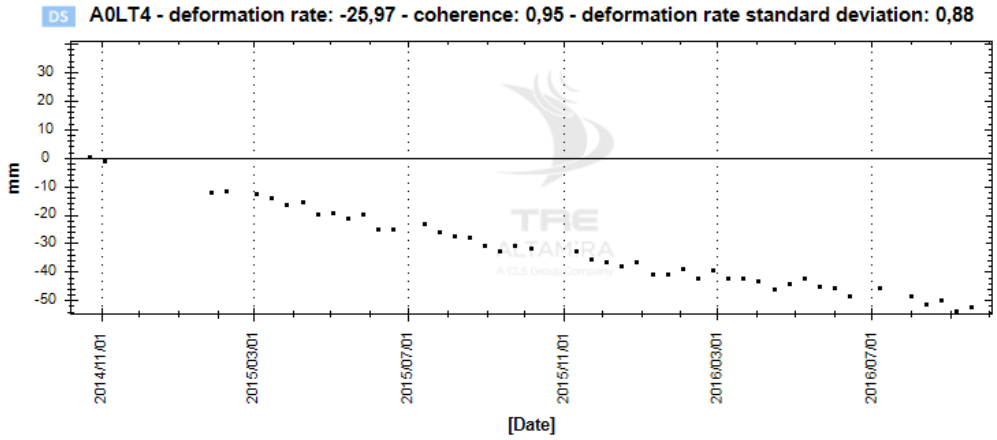

Figure 13: Time series TS5 from the SENTINEL ground deformation analysis

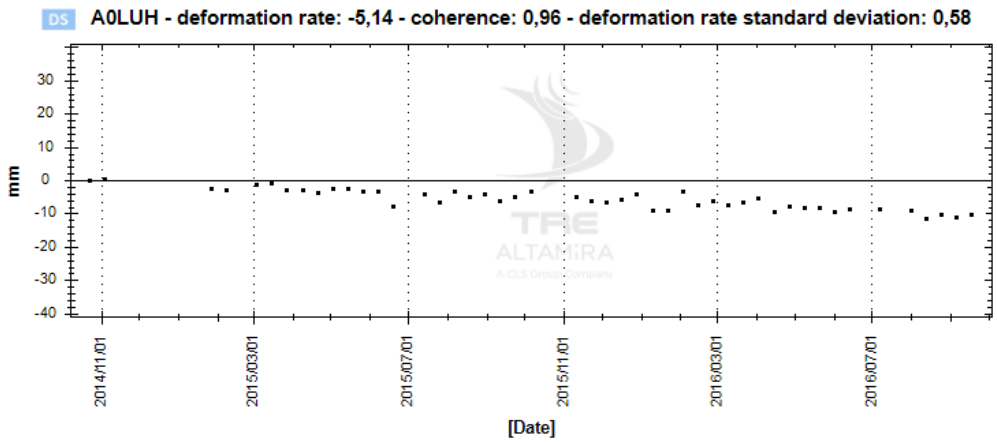

Figure 14: Time series TS6 from the SENTINEL ground deformation analysis.

- **Cosmo-SkyMed (October 2016 to February 2017).**

Over 129061 unique PS points and DS points representing line-of sight movements were identify from a SqueeSAR analysis. The figure 15 shows the accumulated displacement map during the period October 2016 to February 2017 obtained with Cosmo-SkyMed satellites data. The accumulated displacement during 120 days is presented in every point obtained and also the spatial distribution of the measures covering a wide area with a high density of measurement points. The value scale is set between 30 to -30 mm (1.18 inches).

Higher motion magnitudes are detected just in the perimeter and surrounding of the sinkhole areas showing more than 100 mm (3.93 inches) of accumulated motion in approximately 3 months of study. The time series shown in fig 16 shows the linear evolution of the motion and a slight acceleration at the beginning of November 2016.

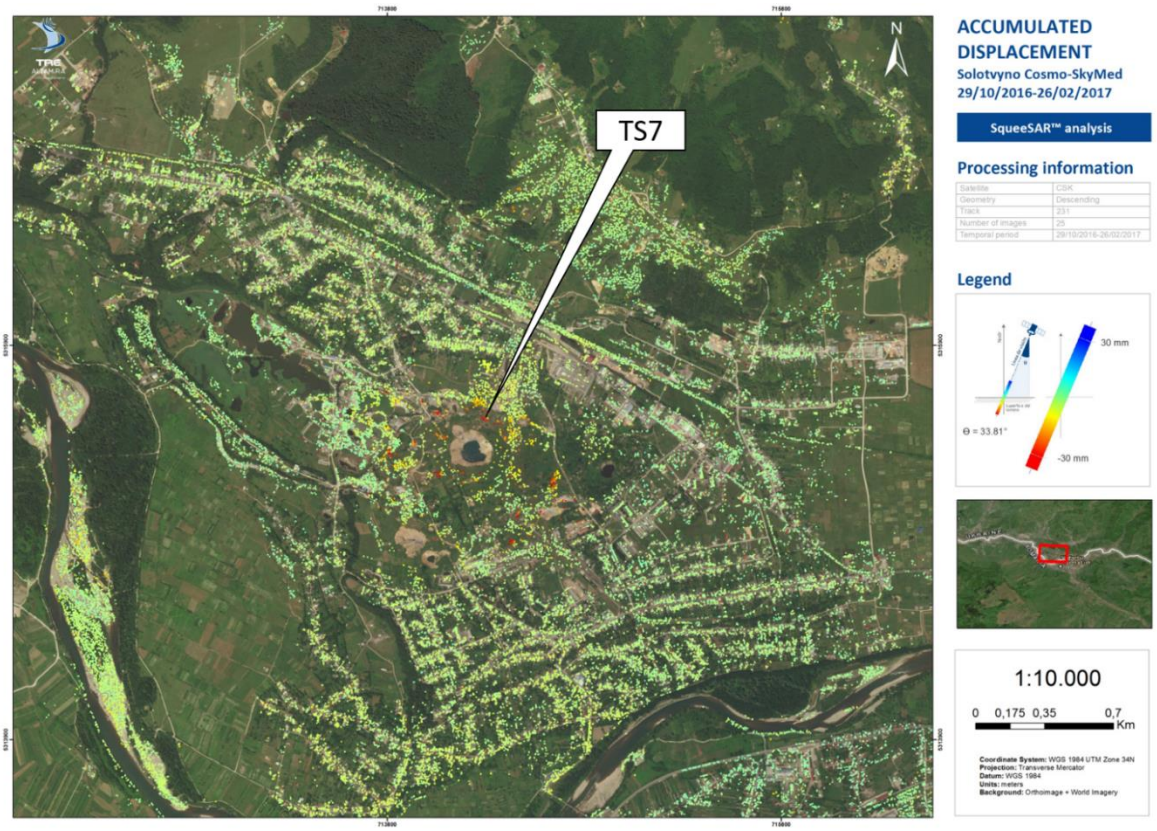

Figure 15: Accumulated deformation map from Cosmo-SkyMed data for the period October 2016 – February 2017.

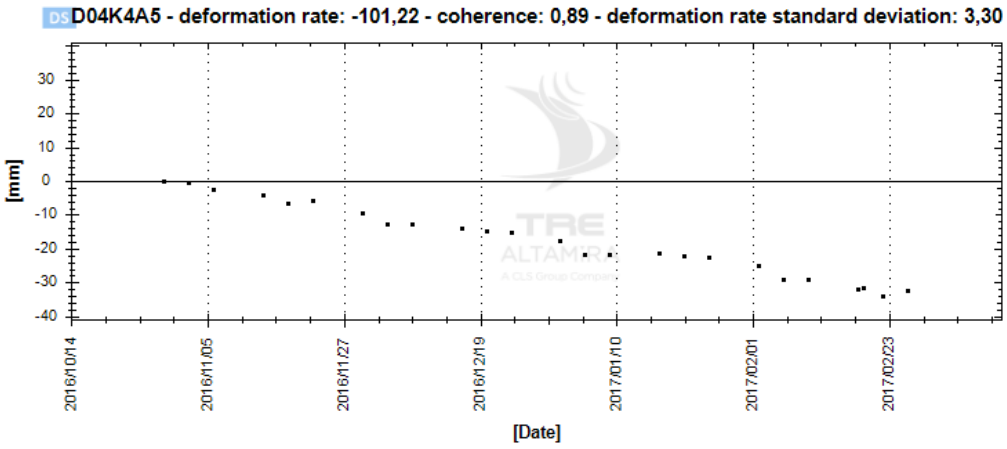

Figure 16: Time series TS7 from the Cosmo-SkyMed ground deformation analysis

3.2. Sinkhole and Landslides Risk results

This analysis resulted in the estimation of subsidence and landslide risk within the AOI, considering the evolution of the risk in time. The methodology for estimating risk zones was the following:

- Step 1. Delineation and classification of subsidence and landslide risks for each period of study, namely 1997-2001, 2003-2010 and 2014-2016. The estimation of the average velocity was done for a subset of the available PSs, using only scatterers with velocity > -5mm/yr (0.19 inches/yr). For an average velocity in the range of [-5 -7.5 mm/yr] (-0.19 – 0.29 inches/yr), the corresponding risk zone attributed was LOW and was given a risk level of 1. For an average velocity in the range [-7.5 -15 mm/yr] (0.29 – 0.59 inches/yr) the risk zone attributed was MODERATE and the associated risk level was 2, while for velocities below -15mm/yr (0.59 inches/yr) the polygon is at HIGH risk with a risk level of 3.

-Step 2. Separation of subsidence and landslide risks, based on the underlying slope values (estimated from the DEM). For slopes above 15%, the corresponding polygon was characterized as landslide risk zone; while for slopes below 15% the corresponding polygon was characterized as subsidence risk zone.

The results of applying steps 1 & 2 above are shown in Figure 17e 17.

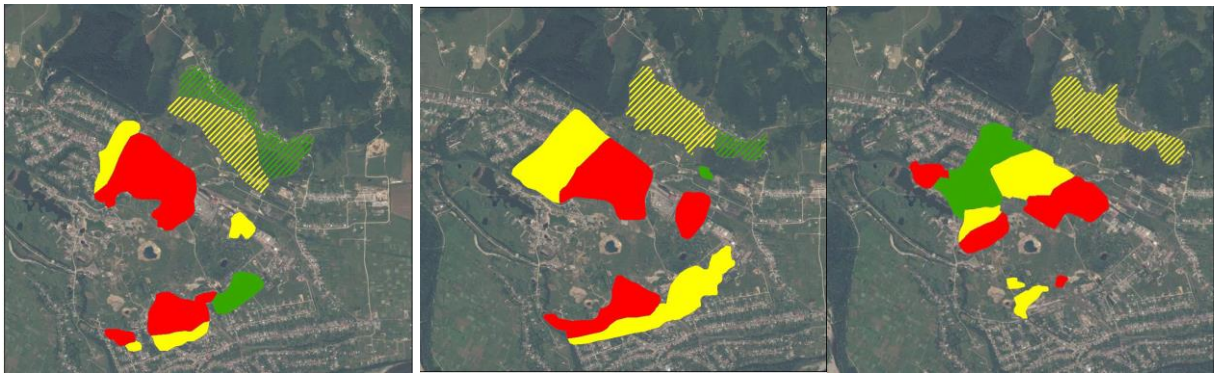

Figure 17. Subsidence and landslide risk zones for the (left) 1997-2001, (middle) 2003-2010 and (right) 2014-2016 periods. Filled polygons correspond to subsidence risk zones, while hatched polygons to landslide risk zones.

-Step 3. An integrated product was then formed to estimate current risk levels (RL), after applying a weighting to the three datasets. The formula used is as follows:

$$Risk\ Level = 67\% \times RL_{2014-2016} + 25\% \times RL_{2003-2010} + 8\% \times RL_{1997-2001}$$

This formula acknowledges that the more recent measurements, i.e. the 2014-2016 Sentinel-1, are more relevant for estimating the current risk levels, and hence are more heavily weighted.

-Step 4. The above algebraic formulation generated a float Risk Level value for several sub-polygons. Values below 0.75 were characterized as low risk, values in the range [0.75-2] as moderate risk and values in the range [2-3] as high risk.

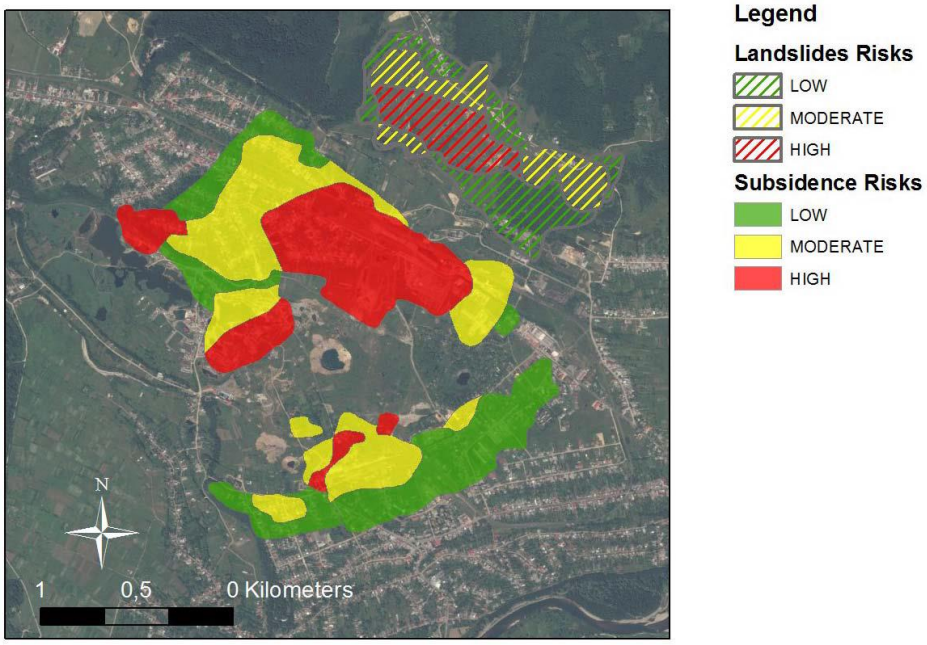

Figure 5. Integrated subsidence and landslide risks for the AOI, using PSI analysis data spannnig from 1997 to 2016.

It is important to note that the absence of any risk polygon in the AOI can mean two things: a) either there was no velocity measurement and therefore we cannot make any assumption on the underlying risk (this is especially applicable for the mining area in the center of the AOI) or b) the velocity values during the delineation phase were above -5 mm/yr (0.19 inches/yr) and therefore the risk is zero (this is especially applicable for the urban area in the south – southeast of the AOI).

-Step 5. The final process in this workflow was overlaying the risk estimation layer with the assets that were mapped using the VHR optical imagery. The statistical information that was extracted is shown in Table 2.

Assets at subsidence risk	**Subsidence Risk Level**		
Built-up areas (sqkm)	**Low**	**Medium**	**High**
Residential	0,82	0,64	0,45
Commercial	0,63	0,63	0,49
Industrial	0,35	0,52	0,39
POIs (Nr)	**Low**	**Medium**	**High**
Airport	-	-	-
Commercial, Public & Private Services	79	44	99
Industry & Utilities	9	13	16
Places of Worship	-	2	-
Other	391	441	249

Assets at landslide risk	**Landslide Risk Level**		
Built-up areas (sqkm)	**Low**	**Medium**	**High**
Residential	0,10	0,05	-
Commercial	-	0	-
Industrial	0	-	-
POIs (Nr)	**Low**	**Medium**	**High**
Airport	-	-	-
Commercial, Public & Private Services	-	-	-
Industry & Utilities	-	-	-
Places of Worship	-	-	-
Other	34	12	-

Table 2. Statistical information on the assets at risk within the AOI for the 1997-2016 analysis

A similar procedure was followed for the estimation of the subsidence and landslide risk using the VHR Cosmo-SKyMed data that were tasked for October 2016 to February 2017.

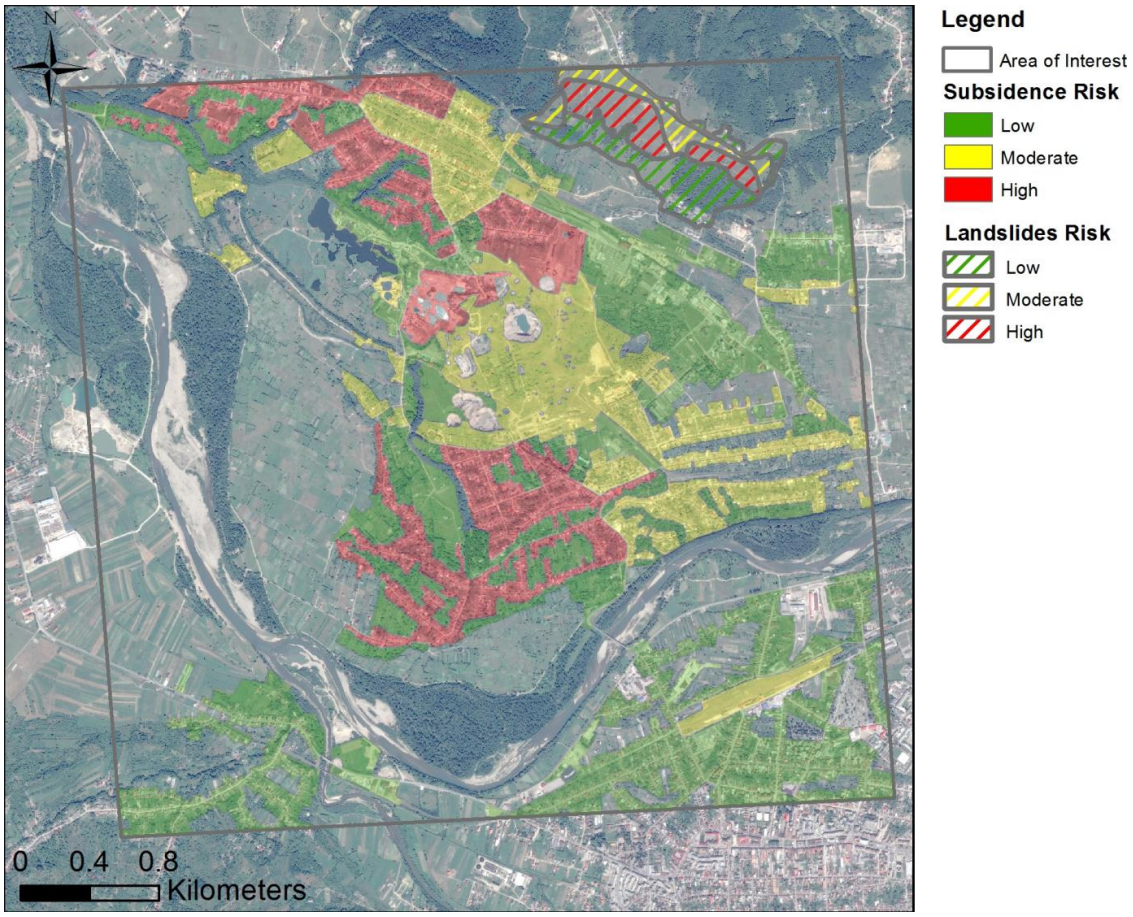

Figure 6. Integrated subsidence and landslide risks for the AOI, using VHR PSI analysis data spannnig from October 2016 to February 2017.

4. Discussion and Conclusions

The results achieved in the Solotvyno AOI provide an indication of the potential of advances InSAR techniques for contributing to the sinkhole and landslides risk assessment related with mining activities.

The InSAR analysis provides a high density of measurements points of ground motion with millimetric precision over the entire Area of Interest for the different periods of time considered.

As it can be seen in the foregoing section, the density of points is not homogenous over the entire AOI because it depends on the ground cover: over high correlated areas, as rock outcrops, the density is higher than over vegetated areas, where surface changes quickly between satellite acquisitions. Furthermore, there is a lack of measurements points over the area around the sinkhole due to the decorrelation of the signal during the entire period under study.

In order to overcome these drawbacks, for covering the last period, a high-resolution satellite (X-band) such as Cosmo-SkyMed, dealing with a much shorter period (4 months) with very frequent revisiting time have been used.

As result, new data around the sinkhole were obtained, showing an accumulated displacement up to 100 mm (3.93 inches). Additionally, it can be seen that due to the better spatial resolution (please, see Table

1) that provide this satellite in comparison with the C-band satellites, the density of points has increased significantly.

The resulting InSAR results served as input for delimitating the subsidence and landslide risk areas. For the period 1997-2016 risk was estimated using high resolution C-band data, while for October 2016 to February 2017 the risk was assessed based on very high resolution (both spatial and temporal) X-band data. For both analysis periods, the spatial pattern of landslide risk is quite similar, where at the northeast of the AOI a high risk zone is identified in both cases. Considering subsidence risk near the mining areas, the very high resolution (VHR) Cosmo-SkyMed data showcase their superiority. Firstly, X-band data provide meaningful risk information in the center of the AOI where most of the mining sites lay; this is the same location where there is an information gap for the C-band data. Such discrepancy is mainly attributed to the frequent SAR acquisitions in the respective data stack. Secondly, the spatial detail of the risk variations within Soltvyno's urban fabric is much higher in the second processing period (2016-2017), highlighting the value of VHR SAR data. Overall, considering the results of the overall risk analysis, we identified several assets, including predominantly habited areas, of being at moderate and high risk zones as the result of the mines' underground physical processes. In Solotvyno, about 2.9 km^2 (3.5 million $yards^2$) of residential, commercial and industrial zones are at relatively high risk zones considering the sinkhole generation history of the area. Such information is of paramount importance for the local stakeholders and decision makers that need to analyze and draft a plan for developing mitigation measures and disaster recovery scenarios.

Acknowledges

This study was elaborated in the framework service contract N. 259811, for the Risk & Recovery leg of the Copernicus Emergency Management Service, on behalf of the Hungarian National Directorate General for Disaster Management that participated to the Scoping Mission in Solotvyno mine.

We also would like to acknowledges the contribution of Carles Couso and Maite García in the elaboration of this work.

References

Adam, N, Parizzi, A & Crosetto, M 2009, 'Practical Persistent Scatterer Processing Validation in the Course of the Terrafirma Project', Journal of Applied Geophysics, vol. 69, pp. 59–65.

Berardino, P., Fornaro, G., Lanari, R., Sansosti, E. (2002). "A new algorithm for surface deformation monitoring based on small baseline differential SAR interferograms". IEEE Transactions on Geoscience and Remote Sensing, 40(11), 2375-2383.

Colombo, D., and B. MacDonald. "Using advanced InSAR techniques as a remote tool for mine site monitoring." (2015). The Southern African Institute of Mining and Metallurgy. Slope Stability 2015.

Costantini. M., Minati, F., Ciminelli, M. G., Ferrett,i A., and Costabile, S. 2015. Nationwide ground deformation monitoring by persistent scatterer interferometry. Proceedings of IGARSS 2015, IEEE International Geoscience and Remote Sensing Symposium, Milan, Italy, July 2015. IEEE Geoscience and Remote Sensing Society.

Falorni, G., Morgan, J., Eneva, M. (2011). Advanced InSAR techniques for Geothermal Exploration and Production. GRC Transactions, Vol 35.

Ferretti, A. (2014). Satellite InSAR Data – Reservoir Monitoring from Space. EAGE Publications, Houten, The Netherlands.

Ferretti, A., Fumagalli, A., Novali, F., Prati, C., Rocca, F., and Rucci, A. (2011). A new algorithm for processing interferometric data-stacks: SqueeSAR. IEEE Transactions on Geoscience and Remote Sensing, vol. 49, no. 9. pp. 3460-3470.

Ferretti, A., Prati, C., and Rocca, F. (2001). Permanent scatterers in SAR interferometry. IEEE Transactions on Geoscience and Remote Sensing, vol. 39, no. 1. pp. 8 -20.

Garcia, M. 2017. Mapping the derived risks of abandoned mines with InSAR technology. News TRE ALTAMIRA.http://tre-altamira.com/news/mapping-derived-risks-abandoned-mines-insar-technology. Accessed 21st of August of 2017.

Graniczny, M; Kowalskym Z; Przylucka, M; Colombo, D. 2013. How satellites help the polish mining industry in detecting coal mining induced surface deformation. Reprinted from the World Coal. August 2013.

Massonnet, D and Feigl, K L, 1998, “Radar interferometry and its application to changes in the Earth's surface”, in Rev. Geophys., 36(4), 441–500, doi: 10.1029/97RG03139.

Melchers, C. 2017. Research activities for global post-mining challenges. Conference proceedings. Mining Forum. Berlin (Germany), 1-2 June 2017.

Paradella, W. R., Ferretti, A., Mura, J. C., Colombo, D., Gama, F. F., Tamburini, A., & Silva, A. Q. (2015). Mapping surface deformation in open pit iron mines of Carajás Province (Amazon Region) using an integrated SAR analysis. Engineering Geology, 193, 61-78.

Pinto, C., Sánchez, C., Carneiro, S., De Matos, B. (2017). O uso da tecnologia InSAR (Interferometria de radar de abertura sintéica) para o monitoramento da estabilidade de barragens. Proceedings of the XXXI Seminário Nacional de Grandes Barragens 2017 (XXXI National Seminar on Large Dams), Belo Horizonte (Brasil).

Przyłucka, M., Herrera, G., Graniczny,M., Colombo, D ., Béjar-Pizarro, M. (2015). Combination of Conventional and Advanced DInSAR to Monitor Very Fast Mining Subsidence with TerraSAR-X Data: Bytom City (Poland). Remote Sensing ISSN 2072-4292

Raventós, J., Arroyo, M., García Guerra, J.M., Conde, A., Salvà, B. and García, M. (2017). “The use of InSAR data to monitor slope stability of dams and water reservoirs”. 85th Annual Meeting of International Comission on Large Dams, Prague, Czech Republic.

Sánchez, F., Conde, A., Salvà, B. and Colombo, D. (2016a). “Use or SAR radar satellite data to measure ground deformation in underground and open pit mine sites, El Teniente case study, Chile”. APSSIM Conference Australian Centre for Geomechanics 2016, Perth, Australia – PM Dight (ed.).

Sánchez, F., Monells, D., Manso, A. and Farías, E, (2016b). “Aplicación de metodología InSAR en la detección de deformaciones en el cráter de subsidencia y entorno minero. Caso de Estudio: Codelco Mina Andina”. 1st International Conference of Underground Mining, Santiago Chile.

Werner, C., Wegmüller, U., Strozzi, T., Wiesmann, A. (2003). “Interferometric point target analysis for deformation mapping”. Proceedings of IGARSS 2003, 4362-4364.